Title

Selective [1,4]-Hydrovinylation of 1,3-Dienes with Unactivated Olefins Enabled by Iron Diimine Catalysts

Journal

Journal of the American Chemical Society, 140(9)

ISSN

0002-7863

Authors

Schmidt, Valerie A
Kennedy, C Rose
Bezdek, Máté J
et al.

Publication Date

2018-03-07

DOI

10.1021/jacs.8b00245

Peer reviewed

HHS Public Access

Author manuscript

J Am Chem Soc. Author manuscript; available in PMC 2019 March 07.

Published in final edited form as:

J Am Chem Soc. 2018 March 07; 140(9): 3443–3453. doi:10.1021/jacs.8b00245.

Selective [1,4]-Hydrovinylation of 1,3-Dienes with Unactivated Olefins Enabled by Iron Diimine Catalysts

Valerie A. Schmidt[†], **C. Rose Kennedy**, **Máté J. Bezdek**, and **Paul J. Chirik**[*]

Department of Chemistry, Princeton University, Princeton, New Jersey 08544, United States

Abstract

The selective, intermolecular [1,4]-hydrovinylation of conjugated dienes with unactivated α-olefins catalyzed by α-diimine iron complexes is described. Value-added "skipped" diene products were obtained with exclusive [1,4]-selectivity, and the formation of branched, (*Z*)-olefin products was observed with no evidence for alkene isomerization. Mechanistic studies conducted with the well-defined, single-component iron precatalyst (^{Mes}DI)Fe(COD) (^{Mes}DI =[2,4,6-Me_3-C_6H_2-N=CMe]$_2$); COD = 1,5-cyclooctadiene) provided insights into the origin of the high selectivity. An iron diene complex was identified as the catalyst resting state, and one such isoprene complex, (^{iPr}DI)Fe(η^4-C_5H_8), was isolated and characterized. A combination of single crystal X-ray diffraction, Mößbauer spectroscopy, magnetic measurements, and DFT calculations established that the complex is best described as a high-spin Fe(I) center (S_{Fe} = 3/2) engaged in antiferromagnetic coupling to an α-diimine radical anion (S_{DI} = −1/2), giving rise to the observed S = 1 ground state. Deuterium-labeling experiments and kinetic analyses of the catalytic reaction provided support for a pathway involving oxidative cyclization of an alkene with the diene complex to generate an iron metallacycle. The observed selectivity can be understood in terms of competing steric interactions in the transition states for oxidative cyclization and subsequent β-hydrogen elimination.

Graphical abstract

[*]Corresponding Author: pchirik@princeton.edu.

[†]Present Addresses: Department of Chemistry and Biochemistry, UC San Diego; La Jolla, CA 92093, USA

Notes

The authors declare no competing financial interest.

Supporting Information

The Supporting Information is available free of charge via the internet at http://pubs.acs.org.

Crystallographic information for (^{iPr}DI)Fe(η^4-C_5H_8) and ^{cyp}DIFe(COD) (CIF)

Experimental details; characterization data including NMR spectra of novel compounds; Mößbauer spectroscopic data; kinetic data; computational methods and results (PDF)

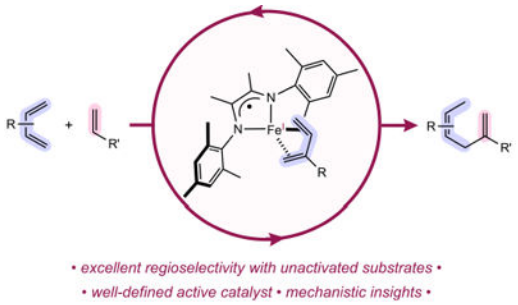

INTRODUCTION

Ethylene and downstream linear α-olefins derived from petrochemical sources and biomass number among the most abundant building blocks for synthesis and constitute core organic base stock for many products of the chemical industry.[1] The development of vast shale gas reserves has increased domestic ethylene production to record-setting levels with supply often exceeding manufacturing polymerization capacity.[2] Production of linear α-olefins, specifically 1-hexene and 1-octene, from selective oligomerization of ethylene has also undergone rapid expansion.[3] Catalytic methods that transform these abundant alkenes into new hydrocarbon architectures and other value-added products are therefore desirable.

Hydrovinylation reactions are atom-economical methods for upgrading commodity hydrocarbons.[4,5] Structural complexity is increased in a single step, and the resulting products offer differentiated alkene functionality amenable to subsequent elaboration.[5] Key challenges for catalyst development include the control of chemo-, regio- and stereoselectivity. Examples of metal-catalyzed reactions for the hydrovinylation of 1,3-dienes date to reports from Hata[6] and from Iwamoto and Yuguchi[7] wherein treatment of butadiene (**1a**) with high pressures of ethylene (**2a**), iron salts, and organoaluminum activators produced low yields of isomeric coupling products (Scheme 1A).[8] Subsequent optimization studies identified more robust iron[9] and cobalt[10] compounds with bis(phosphine) ligands to achieve the same transformation with improved yield and shorter reaction times. Hilt,[11] RajanBabu,[12] and others have independently advanced these reactions with cobalt bis(phosphine) complexes to promote [1,4]-hydrovinylation of a range of dienes with alkenes under mild conditions (Scheme 1B). In some cases, ligand modification altered the sense of regioselectivity with unsymmetric substrates (branched vs. linear, C1 vs. C4 C–C bond formation).[11,13] High enantioselectivity has been achieved for the hydrovinylation of substitutionally varied 1,3-dienes with ethylene[12a–e] or acrylate esters.[12f] Separately, Ritter and coworkers reported that pyridine-2-imine-supported iron complexes promoted linear-selective hydrovinylation with styrenes (Scheme 1B).[14] Nickel[15,16] and ruthenium[17] catalysts with NHC or phosphorus-based ligands are also known to effect the homodimerization of 1,3-dienes[15] as well as the [1,2]-hydrovinylation of alkenes and 1,3-dienes.[16,17]

Despite these advances, methods for the selective synthesis of the various “skipped” dienes (1,4-dienes) available from hydrovinylation of commodity hydrocarbons remain underdeveloped. Specifically, branched regioisomers arising from C–C bond formation

between the Cβ position of an α-olefin and the C1 position of an unsymmetric diene are inaccessible using current methods. Rational catalyst evolution and improvement has been limited by a lack of mechanistic insight. State-of-the-art hydrovinylation methods (Scheme 1B) typically rely on the in situ activation of metal–ligand combinations with reducing agents such as Mg, Zn, NBu_4BH_4, or MAO (MAO = methylaluminoxane).[11-14] RajanBabu and coworkers have characterized cobalt(I) precatalysts that did not require activation by a reductant.[12f] However, these complexes required the addition of $NaB(Ar^F)_4$ (Ar^F = 3,5-bistrifluoromethylphenyl) to promote catalysis, and the isolation of on-cycle species was not reported.[12f] Beyond this example, no concrete mechanistic insight has been described about the identities, speciation, and oxidation states of metal complexes responsible for C–C bond formation in the [1,4]-hydrovinylation of dienes.

Reduced, aryl-substituted pyridine(diimine)iron complexes are highly effective catalysts for numerous C–C bond-forming reactions with unactivated alkenes as substrates,[18] including the regioand diastereoselective intra-[19] and intermolecular[20] [2+2]-cycloaddition of α-olefins (Scheme 2A, top). Catalytically competent intermediates have been isolated, and their electronic structures, which involve participation of the redox-active pyridine(diimine) ligand, have been elucidated.[21-23] The reaction proceeds through an Fe(I)/Fe(III) cycle involving oxidative coupling of two alkenes to form a five-membered metallacycle (Scheme 2A, inset). In this mechanism, both the intermediate bis-olefin complex (not shown) and metallacycle (Scheme 2A, inset) have $S = 1$ ground states, and the pyridine(diimine) maintains its one-electron reduced, radical form throughout.[21]

Selective cross-[2+2]-cycloaddition reactions of alkenes and dienes have also been observed using pyridine(diimine)iron catalysts (Scheme 2B).[20,24] In this case, the sequence initiates from an $S = 0$ pyridine(diimine) iron butadiene complex (not shown), with an unusual s-*trans* diene configuration.[19,24] Reversible ethylene insertion generates a diamagnetic iron allyl–alkyl metallacycle (Scheme 2B, inset) that undergoes butadiene-induced reductive elimination to liberate the vinylcyclobutane product.[24] The metallacycle, which has been characterized crystallographically, is best described as a closed-shell Fe(II)–Fe(IV) hybrid with the redox noninnocent pyridine(diimine) functioning as a classical π-acceptor.[23,24] The differing ground-state electronic structures observed experimentally for these two systems (alkene–alkene vs. alkene–diene coupling) have been corroborated by CASPT2/DFT analysis.[25]

These observations suggested that catalyst control could be used to leverage the reactivity of metallacycles formed from alkene–diene coupling to favor hydrovinylation rather than [2+2]-cycloaddition. Specifically, we reasoned that less sterically encumbered coordination environments would disfavor $C(sp^3)$–$C(sp^3)$ reductive elimination and open pathways for β-hydrogen elimination followed by C–H reductive elimination to yield acyclic products (Scheme 2C). Lending credence to this hypothesis, a pyridine(diimine) iron catalyst bearing a single 2-aryl substituent, ($^{2\text{-}tBu}$PDI)$FeCH_3$, produced 2,3-dimethylbutene as the major product of propylene dimerization (Scheme 2A, bottom). [20] This product likely derives from the same metallacycle that led to 1,2-dimethyl cyclobutane with more sterically hindered catalysts.

By virtue of their open coordination sites and analogy to the pyridine(diimine) iron complexes responsible for [2+2]-cycloaddition reactions, reduced iron complexes bearing redox-active bidentate ligands were identified as promising candidates for selective catalysis of alkene–diene hydrovinylation. Seminal reports from Takacs[26] and tom Dieck[27] introduced the use of such ligands for diene coupling reactions, and Ritter and coworkers applied pyridine-2-imine-supported iron complexes for linear-selective hydrovinylation using styrenes (Scheme 2A).[14] However, extension of the method beyond styrenes and allylbenzene has not been realized. Related bidentate α-diimine ligands were targeted for our investigation of iron-catalyzed hydrovinylation given their ease of preparation, modularity, well-established redox activity,[28] and precedent in iron catalysis.[27,29,30] Here we describe the synthesis and electronic structure studies of α-diimine iron diene complexes that are highly active for the hydrovinylation of dienes with unactivated alkenes with nearly exclusive [1,4]-selectivity using equimolar ratios of substrates (Scheme 3). Kinetic studies, deuterium-labeling experiments, and the isolation of intermediates allowed identification of a resting-state iron diene complex bearing a redox-active α-diimine ligand that supports a mechanism involving oxidative coupling with alkenes to form on-cycle metallacyclic intermediates. Comparison of the electronic structure of catalytically relevant diimine iron complexes to related pyridine(diimine) iron complexes is also presented, highlighting the prevalence of ligand-centered radicals in Fe-catalyzed carbon–carbon bond-forming chemistry.[18b]

RESULTS AND DISCUSSION

Method Development and Catalyst Optimization

The development of a method for intermolecular, iron-catalyzed diene hydrovinylation was explored initially using myrcene (**1b**) and 1-hexene (**2d**) as coupling partners (Table 1). These specific substrates were selected because both are commodity chemicals available from petrochemical feedstocks[1] or biomass,[31] and both are easily-handled liquids at room temperature.

As described previously, [(^{Me}PDI)Fe(N_2)]$_2$(μ^2-N_2) (^{Me}PDI = 2,6-(2,6-Me_2-C_6H_3-N=CMe)$_2$$C_5H_3N$) promoted efficient cross-reactivity of myrcene and 1-hexene but furnished a near 1:1 mixture of [1,4]-hydrovinylation (**3bd** and **4bc**) and [2+2]-cycloaddition (**5bd**) products.[20,24] To improve selectivity for hydrovinylation, the α-diimine iron olefin complexes (^{iPr}DI)Fe(COE) (^{iPr}DI = [2,6-^{i}Pr_2-C_6H_3-N=CMe]$_2$; COE = cyclooctene) and (^{iPr}DI)Fe(COD) (COD = 1,5-cyclooctadiene) were explored. These compounds were first synthesized by our laboratory for application in alkene hydrogenation,[29] and a related example, (^{Me}DI)Fe(COD), was reported by Ritter as a catalyst for the [4+4] homodimerization of butadiene with very high turnover numbers.[30] Both (^{iPr}DI)Fe(COE) and (^{iPr}DI)Fe(COD) offered improved selectivity for hydrovinylation relative to the pyridine(diimine)iron catalyst, generating **3bd** as the major product with decreased amounts of [2+2]-cycloaddition product **5bd**. Because the 1,5-cyclooctadiene iron compounds are more straightforward to prepare and handle, these were selected for additional catalyst evaluation studies.

The effect of 2,6-aryl substituents on the α-diimine catalysts was evaluated for the hydrovinylation of myrcene with excess 1-hexene (Table 1). The least sterically encumbered iron complex in the series, (^{Mes}DI)Fe(COD), was the most selective, affording complete chemoselectivity for hydrovinylation, excellent regioselectivi-ty (95:5 *C1, branched : C4, branched*), and exclusive formation of the (*Z*)-olefin isomer. Increasing the size of the 2,6-aryl substituents decreased selectivity for hydrovinylation; precatalysts bearing ethyl or cyclopentyl groups produced small but detectable quantities of the [2+2] cycloaddition product **5bd**. Treatment of $FeCl_2$ with $Mg(C_4H_6)$•2THF in the absence of ligand afforded only trace conversion and yielded a complex mixture of isomeric products.

The regioselectivity obtained with (^{Mes}DI)Fe(COD) complements cobalt-catalyzed methods reported previously that favor the *C4, branched* or *C1, linear* isomers of related products.[11] It is also notable that the catalyst was prepared readily in three straightforward steps: (i) the condensation of inexpensive reagents (diacetyl and 2,4,6-trimethylaniline) to form the diimine, (ii) metalation with an iron(II) halide, and (iii) subsequent reduction with magnesium butadiene in the presence of 1,5-cyclooctadiene (see Experimental Section and Supporting Information).

Regioselective Diene Hydrovinylation

Having identified a highly active and selective iron catalyst for the [1,4]-hydrovinylation of myrcene with 1-hexene, the scope of the reaction with various coupling partners was explored. Butadiene self-dimerization proceeded rapidly in the absence of a suitable cross-coupling partner using (^{Mes}DI)Fe(COD),[30] but the butadiene hydrovinylation products (**3aa–3af**) were formed in high yield using ethylene or an α-olefin with more encumbered (^{iPr}DI)Fe(COD) as the pre-catalyst (Scheme 3, top). By contrast, substituted 1,3-dienes underwent only very slow self-dimerization under standard reaction conditions with (^{Mes}DI)Fe(COD), and these substrates engaged readily in [1,4]-hydrovinylation with ethylene or 1-hexene (Scheme 3, bottom; Scheme 4A). Notably, cross reactivity was observed with equimolar quantities of diene and α-olefin, highlighting the improved activity of this class of catalysts over pyridine(diimine) iron complexes, with which excess alkene was required to suppress diene coupling chemistry.[20]

Dienes bearing substitution at the C2 position exclusively, such as isoprene and myrcene, underwent C–C bond formation at the C1 termini and formed the branched regioisomers arising from coupling at Cβ. The iron-catalyzed reactions were also highly stereoselective; only the *(Z)*-isomers of **3aa–ea, 3bd, 3cd**, and **3ed** were detected. The preference for C–C bond formation at C1 was retained with additional substitution (e.g. products **3ea** and **3ed**), although selectivity for the branched product eroded slightly. In each of these examples, the stereochemical outcome could be justified in terms of steric interactions between a postulated metallacycle and the ligand framework during C–C bond formation, wherein the mechanism for oxidative cyclization would require formation of the *cis*-olefin geometry (vide infra).

The scope of the alkene partner for the iron-catalyzed hydrovinylation reaction was explored using myrcene as a representative diene. Nearly exclusive *C1, branched* selectivity was maintained for a range of linear and branched α-olefins including ethylene (**2a**), propylene

(**2b**), 1-decene (**2f**), allylbenzene (**2g**), and 3-methyl-1-pentene (**2h**). More hindered alkenes—such as 3,3-dimethyl-1-pentene (**2i**), 3-methyl-1-butene (**2j**), 3-methyl-1-pentene (**2k**), vinylcyclobutane (**2l**), citronellene (**2o**), allyltrimethylsilane (**2r**), and vinyltrimethylsilane (**2s**)—were all suitable substrates for the iron-catalyzed hydrovinylation reaction, although longer reaction times (up to 96 h to form **3bo**; see Supporting Information) or neat reaction conditions (for **3bi** and **3bo**) were required for the most hindered cases. Terminal alkenes bearing pendant internal alkenes—such as 4-vinylcyclohexene (**2m**), 5-vinyl-2-norbornene (**2n**), and citronellene (**2o**)—reacted exclusively at the terminal position and thereby introduced sterically and electronically differentiated synthetic handles into the tetra-olefin products. In a notable entry, **3bp** was prepared from 1,5-hexadiene (**2p**). Use of a modest excess (5 equiv) of the bis-olefin generated the [1,4]-hydrovinylation product cleanly, forming only trace levels of side products arising from cycloisomerization or sequential hydrovinylation at both termini.

The *C1, branched* products of hydrovinylation reactions with allyltrimethylsilane (**2r**) and vinyltrimethylsilane (**2s**) offer additional synthetic versatility, as the silyl groups in **3br** and **3bs** may be elaborated to other functionality. Furthermore, the electronically biased vinylboronic acid pinacol ester (**2t**) reacted with myrcene to afford the *C1, linear* product (**6bt**). This product is also poised for diversification by cross coupling or other deborylative transformations to afford access to a suite of hydrovinylation products with regioselectivity complementary to that achieved through the direct reaction of unbiased olefins. The discrepancy in selectivity suggests that different mechanisms may be operative for the hydrovinylation reactions with electron-neutral and electron-deficient olefin coupling partners. Nonetheless, styrene and acrylates, which were the optimal substrates for the pyridine-2-imine iron catalysts described by Ritter,[14] were not reactive under these conditions.

Use of single-component, reduced iron precatalysts, such as (^{Mes}DI)Fe(COD), allowed for the evaluation of intrinsic catalyst activity and selectivity without potential complications from activators and their byproducts. Nonetheless, select hydrovinylation reactions were also conducted using the bench-stable iron(II) halide precatalyst (^{Mes}DI)$FeBr_2$ directly with the addition of magnesium butadiene ($Mg(C_4H_6)$•2THF) as an in situ reductant. No erosion of chemo- or regioselectivity was observed with the in situ activation protocol, and the modified conditions—Et_2O was also added to improve solubility of the iron(II) halide and reductant—allowed for the facile preparation of hydrovinylation products **3bb, 3cb**, and **3cd** on multigram scale (Scheme 5). Altogether, the iron-catalyzed hydrovinylation represents a highly efficient method for achieving rapid structural elaboration of minimally functionalized building blocks to afford value-added “skipped” diene products with high chemo- and regioselectivity.

Kinetic Analysis

Selective 1,4-hydrovinylation promoted by a well-defined, single-component organometallic iron precursor offered the opportunity for mechanistic studies to determine what role the α-diimine played in catalytically relevant intermediates. To establish the nature of the active species responsible for C–C bond formation and for dictating selectivity for hydrovinylation,

a kinetic analysis of a representative reaction was conducted. The hydrovinylation of myrcene (**1b**) with 1-octene (**2e**) was selected as both are easily handled liquid reagents. The progress of the reaction under catalytically relevant conditions (where $[\mathbf{1b}]_0 = [\mathbf{2e}]_0 = 0.5$ M, see Figure 1A; or where $[\mathbf{1b}]_0 = (1/5)[\mathbf{2e}]_0 = 0.5$ M; see Supporting Information) was monitored by gas chromatography over ~5 half lives at 23 °C (Figure 1A). Clean exponential decay of myrcene concentration, [**1b**] and corresponding growth of [**3be**] over time established that the reaction exhibited well-behaved kinetics with no induction period or change in selectivity over time. Accordingly, subsequent analyses to determine the order in each reaction component—approximately zero-order in diene [**1b**], first-order in alkene [**2e**], and first-order in catalyst $[Fe]_{tot}$—were performed using the method of initial rates (Figure 1B–D; see Supporting Information for experimental details).[32]

Synthesis and Electronic Structure of Catalytic Intermediates

The rate law for the catalytic hydrovinylation is most consistent with an α-diimine iron diene complex as the catalyst resting state. Attempts to observe such a compound directly by ^{1}H NMR specroscopy during catalytic turnover were unsuccessful due to line broadening; therefore, independent synthesis of such an intermediate was pursued. The isopropyl-substituted variant of the α-diimine ligand, ^{iPr}DI, was selected for these studies due to its improved crystallinity and slightly diminished reactivity compared to the ^{Mes}DI analog. Treatment of (^{iPr}DI)Fe(COD) with a large excess (20 equiv) of isoprene afforded, following recrystallization from pentane, a red–brown paramagnetic solid identified as the isoprene complex (^{iPr}DI)Fe(η^4-C_5H_8) (Scheme 6A). This complex proved to be catalytically competent for hydrovinylation; exposure of a 5:1 mixture of 1-hexene and isoprene to 5 mol % (^{iPr}DI)Fe(η^4-C_5H_8) yielded **3cd** (34% combined yield; 36:32:31 **3cd : 4cd : 5cd**) after 20 hours at 23 °C with effectively identical selectivity to that obtained with (^{iPr}DI)Fe(COD) under the same conditions (Scheme 6C).

The solid-state structure of (^{iPr}DI)Fe(η^4-C_5H_8) was determined by single crystal X-ray diffraction (Scheme 6B), confirming its identity. In contrast to the s-*trans* diene configuration observed with pyridine(diimine)iron butadiene complexes,[19,24] isoprene adopts an s-*cis* configuration in (^{iPr}DI)Fe(η^4-C_5H_8). It is likely that the s-*cis* geometry, which is typical for transition metal diene complexes,[33] is precluded by bulky tridentate pyridine(diimine) ligands but can be accommodated in the more open coordination environment afforded by a bidentate diimine ligand. Like the bis-olefin complexes (^{iPr}DI)Fe(COD)[29] and (^{Me}DI)Fe(COD),[30] the coordination geometry of the iron diene complex is best described as pseudo-tetrahedral. A solution magnetic moment of 2.5 μ_B was measured for (^{iPr}DI)Fe(η^4-C_5H_8) at 25 °C in benzene-d_6, consistent with an S= 1 ground state.[34]

Distortion in the metrical parameters of a ligand is an established reporter of the redox-activity of a chelate.[35] Specifically, the imine N(1)–C(1) and N(2)–C(2) and backbone C(1)–C(2) bond distances of diimine ligands are most sensitive to changes in to ligand oxidation state.[28,36] The relevant bond metrics for (^{iPr}DI)Fe(η^4-C_5H_8) are compiled in Table 2, where they are compared with the analogous metrics for (^{iPr}DI)Fe(COD),[29] (^{C5H9}DI)Fe(COD), (^{Me}DI)Fe(COD),[30] and average values characteristic of a generic diimine ligand in its

neutral, radical anion, and closed-shell dianion forms.[28] The imine N(1)–C(1) and N(2)–C(2) bond distances (1.343(2) and 1.340(2) Å, respectively) for the isoprene complex are elongated relative to the neutral form of the ligand (1.29 Å), while the backbone C(1)–C(2) bond is contracted (1.419(2) Å vs. 1.47 Å for neutral ligand), suggesting one-electron reduction of the diimine ligand. Conversely, the C(29)–C(30) and C(31)–C(32) bond lengths of the isoprene ligand are minimally perturbed relative to those typical of free dienes (1.330 Å for C=C, 1.455 Å for C–C).[37]

These structural parameters, in combination with the magnetic data, are indicative of a high-spin iron(I) center (S_{Fe} = 3/2) engaged in antiferromagnetic coupling with a diimine ligand radical (S_{DI} = −1/2) accounting for the experimentally observed S = 1 ground state. The zero-field ^{57}Fe Mößbauer data (δ = 0.56 mm/s and $|\Delta E_Q|$ = 1.68 mm/s; Figure 2A, *left*) for the isoprene complex are also consistent with this electronic structure description. Zerofield ^{57}Fe Mößbauer data were also collected for (^{iPr}DI)Fe(COD) (δ = 0.48 mm/s and $|\Delta E_Q|$ = 1.30 mm/s; Figure 2B, *left*) and (^{Mes}DI)Fe(COD) (δ = 0.46 mm/s and $|\Delta E_Q|$ = 0.98 mm/s; see Supporting Information). These data are compiled in Table 3 along with the Mößbauer parameters for related diimine,[28,30] β-diketiminate (nacnac),[38] and pyridine(diimine)[21] complexes for comparison.

Full-molecule density functional theory (DFT) calculations of (^{iPr}DI)Fe(η^4-C_5H_8) and (^{iPr}DI)Fe(COD) were performed using the B3LYP functional[39,40] and either unrestricted Kohn–Sham (UKS)[41] and broken-symmetry (BS) possibilities; geometry optimizations were initiated from the experimental solid-state structure. Use of these DFT methods, especially when coupled to spectroscopic data, is widely precedented for determining the ground-state electronic structures of first-row transition metal complexes with redoxactive ligands.[21,22,28,30,38,42] The calculations converged to broken symmetry (3,1) solutions for both (^{iPr}DI)Fe(η^4-C_5H_8) and (^{iPr}DI)Fe(COD). The computed structures reproduced the experimental Mößbauer parameters adequately (e.g. δ = 0.49 mm/s, $|\Delta E_Q|$ = 2.02 mm/s predicted for (^{iPr}DI)Fe(η^4-C_5H_8)).[42c] The spin delocalization depicted in Figure 2 highlights the participation of the diimine ligand in the electronic structure of the active iron catalyst. The computational results, combined with the spectroscopic and crystallographic data, underscore the similarities between electronic structures of (^{iPr}DI)Fe(η^4-C_5H_8) and (^{iPr}DI)Fe(COD); both 16-electron complexes are comprised of high-spin S_{Fe} = 3/2 iron(I) centers coupled antiferromagnetically to diimine ligand radicals (S_{DI} = −1/2) to afford a net S =1 spin state. These findings are in agreement with Ritter's assignment for (^{Me}DI)Fe(COD).[30] While spin-state changes upon alkene coordination may, in principle, occur en route to product formation, these findings provided compelling support for the involvement of ligand redox activity in the overall catalytic cycle.

Deuterium-Labeling Experiments in Support of a Metallacyclic Intermediate

Following identification and electronic structure determination of the catalyst resting state, the possible intermediacy of a metallacycle in the mechanism of iron-catalyzed hydrovinylation was explored. Several key observations supported this hypothesis. Only *(Z)* olefin products were observed (vide supra); neither the *(E)* isomers nor structural isomers were detected under catalytic conditions (Scheme 7A). Furthermore, when 3-methyl-1,3-

pentadiene (**1e**) was subjected to standard catalytic conditions as a mixture of (*E*) and (*Z*) isomers, only (*E*)-**1e** underwent hydrovinylation with ethylene or 1-hexene to form products **3ea** and **3ed**, respectively (Scheme 4); (*E*)-**1e** was not consumed. This reactivity difference could be attributed to the energetic penalty arising from repulsive $A^{1,3}$ interactions in the s-*cis* conformation of (*Z*)-**1e** (Scheme 7B).[43] Taken together, these observations suggested that a mechanism involving direct [1,4]-addition of an iron hydride across a diene was unlikely. While this "Cossee" mechanism is commonly invoked in many alkene oligomerization and diene telomerization reactions,[44,45] the iron allyl resulting from such a process would be expected to isomerize rapidly prior to olefin insertion, leading to a mixture of isomeric products.

More direct evidence was provided by a series of deuteriumlabeling experiments. Performing the hydrovinylation of myrcene (**1b**) with 2-[$^2H_1$]-oct-1-ene (**2e**-d_1) yielded **3be**-d_1, where the alkene β-deuterium was transferred exclusively to the C4 terminus of the 1,3-diene coupling partner (Scheme 7C). No isotope scrambling arising from competitive chain-walking processes was observed. Based on this pattern of isotopic-labeling, an additional crossover/competition experiment was conducted to distinguish definitively between the Cossee and metallacyclic mechanistic possibilities. This experimental design was introduced independently by Belov et al.[46] and by Bercaw and coworkers[47] in the context of titanium- and chromium-catalyzed ethylene oligomerization, respectively. It has since been widely applied to study the mechanisms accessed with other oligomerization catalysts.[48] The experiment takes advantage of the fact that on-cycle metallacycle formation results in *intra*molecular transfer of hydrogen (or deuterium) from one chain end to the other. In contrast, propagation through a metal hydride, alkyl, or allyl complex in a Cossee mechanism results in the *inter*molecular transfer of hydrogen (or deuterium), thereby affording a statistical mixture of crossover isotopologues. Treatment of isoprene with a 1:1 mixture of ethylene and ethylene-d_4 under catalytic conditions for hydrovinylation produced a mixture of isotoplogues **3ca** and **3ca**-d_4 (Scheme 7D). The crossover products that would arise from the intermediacy of a propagating metal hydride (**3ca**-d_1 and **3ca**-d_3) were not detected by quantitative ^{13}C NMR analysis, and the distribution of isotopologues measured by high resolution mass spectrometry was most consistent with that expected for a mechanism involving metallacycle formation (Scheme 7D). The slight deviation of the isotopologue ratio from 1:1 was further indicative of an inverse, secondary, competition kinetic isotope effect (k_H/k_D = 0.83(11)).[49] Given that β-hydrogen elimination and C–H bond-forming reductive elimination would be expected to afford large, primary kinetic isotope effects, this result supported rate-determining C–C bond formation.[50]

Given the combined evidence of the kinetic characterization, the isotope-labeling analysis, and the stereo- and regiochemical course of the reaction, a mechanism involving on-cycle oxidative cyclization is proposed, as depicted in Scheme 8A. In addition to accounting for the reactivity and selectivity trends observed experimentally, this mechanism likely proceeds through a two-electron redox couple enabled by the participation of the redox-active supporting ligand. An analogous Fe(I)/Fe(III) couple was identified previously for the [2+2] cycloaddition of alkenes, wherein select examples of iron(III) metallacycles supported by the $^{iPr(TB)}$PDI ligand (see Table 1 for structure) were isolated and characterized

spectroscopically.[21] Alternatively, oxidative cyclization may result in single-electron oxidation of *both* the diimine ligand-centered radical and the metal center to afford an Fe(II) metallacycle bearing a neutral diimine ligand.[51] Given that metallacycle formation is rate-determining, these possibilities cannot be distinguished rigorously from the experimental information available for this system.

While the transition-state electronic structure likewise cannot be determined unambiguously from the experimental data available, the general mechanistic pathway provides sufficient context to appreciate the basis for selectivity. To the extent that the regiose-lectivity-determining transition structure resembles the postulated metallacyclic intermediate, the high degree of selectivity observed for formation of *C1, branched* products can be justified based on interactions between the metallacycle and ligand framework (Scheme 8B). Namely, the metallacycle en route to the major product minimizes repulsive steric interactions between the coupling partners (where R" = H) and the ligand. Reversing the regiochemistry of either the diene or olefin coupling partner increases the steric encumberance proximal to the ligand and metal center. This energetic difference is attenuated where R" ≠ H due to the introduction of repulsive gauche butane interactions between the coupling partners, resulting in a modest increase in the formation of the minor *C1, linear* product. Nonetheless, selectivity for C1 vs. C4 addition remains high.

CONCLUDING REMARKS

In summary, well-defined single-component iron precatalysts for the selective [1,4]-hydrovinylation of conjugated dienes with α-olefins have been discovered. The products obtained from this method address a major deficiency in regiocontrol among reactions developed to date for the hydrovinylation of 1,3-dienes. An iron diene complex was identified as the resting state and structurally characterized. Determination of the electronic structures of the precatalyst and the resting state established the role of the redoxactive α-diimine ligand, wherein the catalytically active species is best described as an iron(I) center antiferromagnetically coupled to an α-diimine ligand radical anion. Isotopic-labeling studies, kinetic analyses, and structure–reactivity–selectivity relationships provided evidence for a mechanism wherein oxidative cyclization to form an intermediate metallacycle is followed by β-hydrogen elimination. The mechanistic parallels between this system and those described previously for the [2+2] cycloaddition of olefins highlight the general efficacy of these modular iron catalysts for elaborating simple hydrocarbon building blocks to generate value-added structures with excellent and tunable selectivity.

EXPERIMENTAL SECTION[52]

Synthesis of (^{Mes}DI)Fe(COD)

In an N_2-atmosphere glovebox, a 20-mL scintillation vial was charged with ^{Mes}DI (500 mg, 1.55 mmol, 1.0 equiv),[53] iron(II) bromide (333 mg, 1.55 mmol, 1.0 equiv), and a PTFE-coated magnetic stir bar. Tetrahydrofuran (15 mL) was added, and the vial was sealed with a PTFE-lined screw cap. The reaction mixture was maintained with vigorous stirring at ambient temperature (23 °C) as the reaction mixture developed a deep red/purple hue. After 16 hours, the solvent was removed in vacuo. The solid was resuspended in diethyl ether (15

mL) and collected by vacuum filtration over a glass frit, rinsing with additional diethyl ether (3 × 5 mL) until the rinses ran clear. The purple solid (html hex color code #524c59, 758 mg, 91% yield) was dried in vacuo. ^{1}H NMR (CD_2Cl_2, 300 MHz) δ = 116.85 (6H), 15.25 (6H), 7.46 (12H), 2.58 (4H) ppm.

In an N_2-atmosphere glovebox, a 50-mL round bottom flask was charged with (^{Mes}DI)$FeBr_2$ (400 mg, 0.75 mmol, 1.0 equiv) and a PTFE-coated magnetic stir bar. Diethyl ether (8 mL) and 1,5-cyclooctadiene (0.3 mL, 2.4 mmol, 3.3 equiv) were added. The mixture was frozen in a cold well chilled with liquid N_2 for >15 minutes before $Mg(C_4H_6)$•2THF (196 mg, 0.88 mmol, 1.2 equiv)[54] was added in one portion. The flask was sealed with a greased glass stopper, which was secured with a Keck clamp, and returned to the cold well. The reaction flask was maintained in the cold well for 1 hour as it gradually warmed. After 1 hour, the flask was removed from the cold well, and the reaction mixture was stirred vigorously at ambient temperature (23 °C) for two additional hours. The dark purple reaction mixture developed a green/brown hue within 45 minutes. After 3 hours in total, Celite (2 g) was added directly to the reaction flask, and the solvent was removed in vacuo. The dry Celite was transferred to a glass frit and washed with pentane (60 mL). In the receiving flask, the filtrate was concentrated to afford a sticky brown solid. The solid was redissolved in pentane (10 mL), and the solvent was removed in vacuo. This process was repeated to remove excess 1,5-cyclooctadiene until the resulting residue was a brown solid. The crude material was recrystallized from pentane at −35 °C overnight and dried in vacuo to afford an olive solid (html hex color code #3F3F00, 218 mg over two crops, 60% yield). ^{1}H NMR (C_6D_6, 300 MHz) δ = 295.65 (4H), 6.96 (6H), 5.26 (12H), −7.00 (4H), −59.24 (4H), −173.98 (4H), −240.25 (6H) ppm. Elemental analysis calculated for $C_{30}H_{40}N_2Fe$: C, 74.37; H, 8.32; N, 5.78. Found: C, 74.68; H, 7.98; N, 5.74. Note that the reduction may also be effected using Na(Hg) as described previously for the synthesis of (^{iPr}DI)Fe(COD);[29] however, this method affords a mixture of (^{Mes}-DI)Fe(COD) and (^{Mes}DI)$_2$Fe.

General Procedure for [1,4]-Hydrovinylation with Gaseous Substrates

In an N_2-atmosphere glovebox, a J-Young NMR tube was charged with (^{iPr}DI)Fe(COD) (0.006 g, 0.01 mmol, 5 mol %) or (^{Mes}DI)Fe(COD) (0.005 g, 0.01 mmol, 5 mol %) as a solution in C_6D_{12}, C_6D_6, or dodecane (0.5 mL). The tube was sealed, removed from the glovebox, frozen in liquid N_2, and evacuated under high vacuum. Butadiene (0.2 mmol, 1 equiv) and ethylene, propylene, or 1-butene (0.2 mmol, 1 equiv) were added to a separate J-Young NMR tube by sequential calibrated gas bulb additions. The combined starting materials were then transferred to the J-Young tube containing the catalyst solution by way of a vacuum transfer tube. The tube was sealed under static vacuum, and gradually warmed to ambient temperature (23 °C). Reaction progress was monitored by ^{1}H NMR analysis. Upon consumption of the substrates, the volatiles were transferred by way of a vacuum transfer tube to a new J-Young tube for product analysis.

General Procedure for [1,4]-Hydrovinylation with Liquid Substrates

In an N_2-atmosphere glovebox, a 1.5-mL vial was charged with diene 1 (0.5 mmol, 1 equiv), alkene 2 (0.5 mmol, 1 equiv; or 2.5 mmol, 5 equiv), and a PTFE-coated magnetic stir bar. A stock solution of (^{Mes}DI)Fe(COD) (24 mg/10 mL, 0.005 M) was prepared in a 20-mL

scintillation vial, and a portion (1.0 mL, 0.005 mmol, 1 mol %) was transferred to the reaction vial. The vial was sealed with a PTFE-lined screw cap, and the reaction was maintained with stirring at ambient temperature (23 °C) in the glove-box. The reaction was monitored by GC analysis of aliquots removed from the reaction mixture. Upon consumption of the substrates, the vial was removed from the glovebox. The contents were exposed to air and allowed to rest for >1 hour, over which time the deactivated catalyst precipitated from solution. The reaction mixture was filtered through a plug of silica, eluting with pentane (5 × 2 mL), and the filtrate was concentrated under reduced pressure.

Supplementary Material

Refer to Web version on PubMed Central for supplementary material.

Acknowledgments

V.A.S. thanks the NIH for a Ruth L. Kirschstein National Research Service Award (F32 GM109594). M.J.B. thanks the Natural Sciences and Engineering Research Council of Canada for a predoctoral fellowship (PGS-D). Financial support was provided by Firmenich. We thank Dr. Jonathan Darmon and Dr. István Pelczer for helpful discussion.

References

1. (a) Matar, S., Hatch, LF. Chemistry of Petrochemical Processes. 2. Gulf Professional; Boston: 1991. (b) Schmidt, R., Griesbaum, K., Behr, A., Biedenkapp, D., Voges, H-W., Garbe, D., Paetz, C., Collin, G., Mayer, D., Höke, H. Ullmann's Encyclopedia of Industrial Chemistry. Wiley; Chichester, UK: 2014. Hydrocarbons.
2. (a) Short-Term Outlook for Hydrocarbon Gas Liquids. U.S. Energy Information Administration, U.S. Department of Energy; Washington, DC: Mar. 2016 https://www.eia.gov/outlooks/steo/special/supplements/2016/hgl/pdf/2016_sp_01.pdf(b) Short Term Energy Outlook. U.S. Energy Information Administration, U.S. Department of Energy; Washington, DC: Apr. 2017 https://www.eia.gov/outlooks/steo/pdf/steo_full.pdf
3. Ring, K-L., deGuzman, M. Technical Report. IHS Markit; Mar. 2017 Chemical Economics Handbook: Linear Alpha-Olefins. https://www.ihs.com/products/linear-alpha-olefins-chemical-economics-handbook.html
4. (a) Trost BM. Science. 1991; 254:1471–1477. [PubMed: 1962206] (b) Newhouse T, Baran PS, Hoffmann RW. Chem Soc Rev. 2009; 38:3010–3021. [PubMed: 19847337]
5. While hydrovinylation reactions of myriad unsaturated functional groups (e.g. alkynes, alkenes, ketones, etc.) are known, this work focuses specifically on the hydrovinylation of 1,3-dienes. This area has been reviewed: RajanBabu TV. Comprehensive Asymmetric Catalysis. Jacobsen EN, Pfaltz A, Yamamto H. SpringerBerlin1999:417–427. RajanBabu TV. Synlett. 2009:853–885. [PubMed: 19606231] Hilt G. Eur J Org Chem. 2012:4441–4451.
6. (a) Hata G. J Am Chem Soc. 1964; 86:3903–3903.(b) Hata G, Aoki D. J Org Chem. 1967; 32:3754–3758.
7. (a) Iwamoto M, Yuguchi S. Bull Chem Soc Jpn. 1966; 39:2001–2004.(b) Iwamoto M, Yuguchi S. J Org Chem. 1966; 31:4290–4291.
8. Contemporaneous work explored transition metal-catalyzed hydrovinylation of dienes with acrylates under similar conditions: Misono A, Uchida Y, Saito T, Uchida K. Bull Chem Soc Jpn. 1967; 40:1889–1893.
9. Hata G, Miyake A. Bull Chem Soc Jpn. 1968; 41:2762–2764.
10. (a) Hata G, Miyake A. Bull Chem Soc Jpn. 1968; 41:2443–2446.(b) Kagawa T, Inoue Y, Hashimoto H. Bull Chem Soc Jpn. 1970; 43:1250–1251.
11. (a) Hilt G, du Mesnil F-X, Lüers S. Angew Chem Int Ed. 2001; 40:387–389.(b) Hilt F, Lüers S. Synthesis. 2002:609–618.(c) Hilt G, Lüers S, Schmidt F. Synthesis. 2004:634–638.(d) Hilt G,

Danz M, Treutwein J. Org Lett. 2009; 11:3322–3325. [PubMed: 19583205] (e) Arndt M, Reinhold A, Hilt G. J Org Chem. 2010; 75:5203–5210. [PubMed: 20597480] (f) Hilt G, Arndt M, Weske DF. Synthesis. 2010:1321–1324.(g) Hilt G. Synlett. 2011:1654–1659.(h) Hilt G, Roesner S. Synthesis. 2011:662–668.(i) Arndt M, Dindaroğlu M, Schmalz H-G, Hilt G. Org Lett. 2011; 13:6236–6239. [PubMed: 22040103] (j) Erver F, Kuttner JR, Hilt G. J Org Chem. 2012; 77:8375–8385. [PubMed: 22694267] (k) Arndt M, Dindaroğlu M, Schmalz H-G, Hilt G. Synthesis. 2012:3534–3542.

12. (a) Sharma RK, RajanBabu TV. J Am Chem Soc. 2010; 132:3295–3297. [PubMed: 20163120] (b) Page JP, RajanBabu TV. J Am Chem Soc. 2012; 134:6556–6559. [PubMed: 22452442] (c) Timsina YN, Biswas S, RajanBabu TV. J Am Chem Soc. 2014:6215–6218. [PubMed: 24712838] (d) Timsina YN, Sharma RK, RajanBabu TV. Chem Sci. 2015; 6:3994–4008. [PubMed: 26430505] (e) Biswas S, Page JP, Dewese KR, RajanBabu TV. J Am Chem Soc. 2015; 137:14268–14271. [PubMed: 26529467] (f) Jing SM, Balasanthiran V, Pagar V, Gallucci JC, RajanBabu TV. J Am Chem Soc. 2017; 139:18034–18043. [PubMed: 29120629]
13. Cobalt catalysts also effect [1,2]-hydrovinylation of alkenes: Pillai SM, Tembe GL, Ravindranathan M. J Mol Catal. 1993; 84:77–86. Grutters MMP, Müller C, Vogt D. J Am Chem Soc. 2006; 128:7414–7415. [PubMed: 16756275] Bianchini C, Giambastiani G, Meli A, Toti A. Organometallics. 2007; 26:1303–1305. Grutters MMP, van der Vlugt JI, Pei Y, Mills AM, Lutz M, Spek AL, Müller C, Moberg C, Vogt D. Adv Synth Catal. 2009; 351:2199–2208.
14. (a) Moreau B, Wu JY, Ritter T. Org Lett. 2009; 11:337–339. [PubMed: 19093845] (b) McNeill E, Ritter T. Acc Chem Res. 2015; 48:2330–2343. [PubMed: 26214092]
15. For Ni-catalyzed homodimerization of conjugated dienes: Denis P, Jean A, Croizy JF, Mortreux A, Petit F. J Am Chem Soc. 1990; 112:1292–1294. Buono G, Siv C, Peiffer G, Triantaphylides C, Denis P, Mortreux A, Petit F. J Org Chem. 1985; 50:1781–1782.
16. For Ni-catalyzed [1,2]-hydrovinylation of alkenes and conjugated dienes: Kumareswaran R, Nandi M, RajanBabu TV. Org Lett. 2003; 5:4345–4348. [PubMed: 14601996] Zhang A, RajanBabu TV. Org Lett. 2004; 6:1515–1517. [PubMed: 15101781] Zhang A, RajanBabu TV. Org Lett. 2004; 6:3159–3161. [PubMed: 15330612] Zhang A, RajanBabu TV. J Am Chem Soc. 2006; 128:54–55. [PubMed: 16390118] Saha B, RajanBabu TV. J Org Chem. 2007; 72:2357–2363. [PubMed: 17335230] Saha B, Smith CR, RajanBabu TV. J Am Chem Soc. 2008; 130:9000–9005. [PubMed: 18570419] Joseph J, RajanBabu TV, Jemmis ED. Organometallics. 2009; 28:3552–3566. [PubMed: 21532981] Liu W, RajanBabu TV. J Org Chem. 2010; 75:7636–7643. [PubMed: 20964350] Ho C-Y, He LS. Angew Chem Int Ed. 2010; 49:9182–9186. Mans DJ, Cox GA, RajanBabu TV. J Am Chem Soc. 2011; 133:5776–5779. [PubMed: 21449569] Ho C-Y, Chan C-W, He LS. Angew Chem Int Ed. 2015; 54:4512–4516. Lian X, Chen W, Dang L, Li Y, Ho C-Y. Angew Chem Int Ed. 2017; 56:9048–9052. Lian X, Chen W, Dang L, Li Y, Ho C-Y. Angew Chem Int Ed. 2017; 56:9048–9052.
17. (a) He Z, Yi CS, Donaldson WA. Org Lett. 2003; 5:1567–1569. [PubMed: 12713325] (b) He Z, Yi CS, Donaldson WA. Synlett. 2004:1312–1314.(c) Sanchez RP, Connell BT. Organometallics. 2008; 27:2902–2904.
18. (a) Small BL. Acc Chem Res. 2015; 48:2599–2611. [PubMed: 26267011] (b) Chirik PJ. Angew Chem Int Ed. 2017; 56:5170–5181.
19. Bouwkamp MW, Bowman AC, Lobkovsky E, Chirik PJ. J Am Chem Soc. 2006; 128:13340–13341. [PubMed: 17031930]
20. Hoyt JM, Schmidt VA, Tondreau AM, Chirik PJ. Science. 2015; 349:960–963. [PubMed: 26315433]
21. Hoyt JM, Sylvester KT, Semproni SP, Chirik PJ. J Am Chem Soc. 2013; 135:4862–4877. [PubMed: 23448301]
22. For analysis of an analogous catalytic system employing cobalt, see: Schmidt VA, Hoyt JM, Margulieux GW, Chirik PJ. J Am Chem Soc. 2015; 137:7903–7915. [PubMed: 26030841]
23. For discussion of the distinction between ligand redox activity and noninnocence, see: Chirik PJ. Inorg Chem. 2011; 50:9737–9740. [PubMed: 21894966]
24. Russell SK, Lobkovsky E, Chirik PJ. J Am Chem Soc. 2011; 133:8858–8861. [PubMed: 21598972]

25. Note that while the reported ground-state CASPT2/DFT analysis agrees with experimental observations, the transition-state analysis fails to account for the stoichiometry of the ligand-induced reductive elimination step (Ref 24). See: Hu L, Chen H. J Am Chem Soc. 2017; 139:15564–15567. [PubMed: 29063756]
26. Takacs JM, Anderson LG, Madhavan GVB, Creswell MW, Seely FL, Devroy WF. Organometallics. 1986; 5:2395–2398.
27. (a) tom Dieck H, Dietrich J. Chem Ber. 1984; 117:694–701.(b) tom Dieck H, Dietrich J. Angew Chem Int Ed. 1985; 24:781–783.(c) Ehlers J, König WA, Lutz S, Wenz G, tom Dieck H. Angew Chem Int Ed. 1988; 27:1556–1558.(d) Ehlers J, tom Dieck H. Preparation of (1-alkene)-(1,3,-alkadiene) adducts. Ger Offen. 1990 DE 3906434 A1 19900906.
28. (a) Muresan N, Lu CC, Ghosh M, Peters JC, Abe M, Henling LM, Weyhermöller T, Bill E, Wieghardt K. Inorg Chem. 2008; 47:4579–4590. [PubMed: 18442239] (b) Khusniyarov MM, Weyhermöller T, Bill E, Wieghardt K. J Am Chem Soc. 2009; 131:1208–1221. [PubMed: 19105752]
29. Bart SC, Hawrelak EJ, Lobkovsky E, Chirik PJ. Organometallics. 2005; 24:5518–5527.
30. Lee H, Campbell MG, Hernández Sánchez R, Börgel J, Raynaud J, Parker SE, Ritter T. Organometallics. 2016; 35:2923–2929.
31. Behr A, Johnen L. Chem Sus Chem. 2009; 2:1072–1095.
32. The slight inverse dependence of reaction rate on diene concentration, [**1b**]$_0$, may be attributed to reversible formation of an off-cycle complex in which multiple dienes are coordinated to iron. See refs. 27 and 30 for related discussion.
33. Crabtree, RH. The Organometallic Chemistry of the Transition Metals. 5. Wiley; Hoboken, NJ: 2009. p. 132-136.
34. Sur SK. J Magn Reson. 1989; 82:169–173.
35. Eisenberg RE, Gray HB. Inorg Chem. 2011; 50:9741–9751. [PubMed: 21913669]
36. (a) van Koten G, Vrieze K. Adv Organomet Chem. 1982; 21:151.(b) Gardiner MG, Hanson GR, Henderson MJ, Lee FC, Raston CL. Inorg Chem. 1994; 33:2456–2461.(c) Rijnberg E, Richter B, Thiele K-H, Boersma J, Veldman N, Spek AL, van Koten G. Inorg Chem. 1998; 37:56–63. [PubMed: 11670260]
37. Allen FH, Kennard O, Watson DG, Brammer L, Orpen AG, Taylor R. J Chem Soc Perkin Trans. 21987:S1–S19.
38. (a) McWilliams SF, Brennan-Wydra E, MacLeod C, Holland PL. ACS Omega. 2017; 2:2594–2606. [PubMed: 28691111] (b) Dugan TR, Bill E, MacLeod KC, Brennessel WW, Holland PL. Inorg Chem. 2014; 53:2370–2380. [PubMed: 24555749] (c) Cowley RE, Christian GJ, Brennessel WW, Neese F, Holland PL. Eur J Inorg Chem. 2012:479–483.(d) Dugan TR, Bill E, MacLeod KC, Christian GJ, Cowley RE, Brennessel WW, Ye S, Neese F, Holland PL. J Am Chem Soc. 2012; 134:20352–20364. [PubMed: 23181620]
39. Neese F. WIREs Comput Mol Sci. 2012; 2:73–78.
40. (a) Becke AD. Phys Rev A. 1988; 38:3098–3100.(b) Lee CT, Yang WT, Parr RG. Phys Rev B. 1988; 37:785–789.
41. Pople JA, Gill PMW, Handy NC. Int J Quantum Chem. 1995; 56:303–305.
42. (a) Neese F. Inorg Chim Acta. 2002; 337:181–192.(b) Sinnecker S, Slep LD, Bill E, Neese F. Inorg Chem. 2005; 44:2245–2254. [PubMed: 15792459] (c) Römelt M, Ye S, Neese F. Inorg Chem. 2009; 48:784–785. [PubMed: 19102678]
43. (a) Hoffmann RW. Chem Rev. 1989; 89:1841–1860.(b) O'Brien AG. Tetrahedron. 2011; 67:9639–9667.
44. Such a mechanism has been proposed for hydrovinylation reactions catalyzed by cobalt bisphosphine complexes. For example, see ref. 12d. See also: Zingales F, Canziani F, Chiesa A. Inorg Chem. 1963; 2:1303–1304.
45. Hartwig, JF. Organotransition Metal Chemistry: From Bonding to Catalysis. University Science Books; Mill Valley, CA: 2010.
46. Belov GP, Dzhabiev TS, Kolesnikov IM. J Mol Cat. 1982; 14:105–112.

47. (a) Agapie T, Schofer SJ, Labinger JA, Bercaw JE. J Am Chem Soc. 2004; 126:1304–1305. [PubMed: 14759164] (b) Agapie T, Labinger JA, Bercaw JE. J Am Chem Soc. 2007; 129:14281–14295. [PubMed: 17973377]

48. For select applications in the mechanistic investigation of other catalytic systems, see: Tomov AK, Chirinos JJ, Jones DJ, Long RJ, Gibson VC. J Am Chem Soc. 2005; 127:10166–10167. [PubMed: 16028917] Overett MJ, Blann K, Bollmann A, Dixon JT, Haasbroek D, Killian E, Maumela H, McGuinness DS, Morgan DH. J Am Chem Soc. 2005; 127:10723–10730. [PubMed: 16045361] Tomov AK, Chirinos JJ, Long RJ, Gibson VC, Elsegood MRJ. J Am Chem Soc. 2006; 128:7704–7705. [PubMed: 16771461] McGuinness DS, Suttil JA, Gardiner MG, Davies NW. Organometallics. 2008; 27:4238–4247. Tomov AK, Gibson VC, Britovsek GJP, Long RJ, van Meurs M, Jones DJ, Tellmann KP, Chirinos JJ. Organometallics. 2009; 288:7033–7040.McGuinness DS. Organometallics. 2009; 28:244–248.Suttil JA, McGuinness DS, Evans SJ. Dalton Trans. 2010; 39:5278–5285. [PubMed: 20442942] McGuinness DS, Davies NW, Horne J, Ivanov I. Organometallics. 2010; 29:6111–6116.Suttil JA, McGuinness DS, Pichler M, Gardiner MG, Morgan DH, Evans SJ. Dalton Trans. 2012; 41:6625–6633. [PubMed: 22246372] Karpiniec SS, McGuinness DS, Britovsek GJP, Patel J. Organometallics. 2012; 31:3439–3442.Suttil JA, McGuinness DS. Organometallics. 2012; 31:7004–7010.Metzger ED, Comito RJ, Hendon CH, Dinca M. J Am Chem Soc. 2017; 139:757–762. [PubMed: 27966939]

49. Melander, L., Saunders, WH, Jr. Reaction Rates of Isotopic Molecules. Wiley; New York: 1980.

50. In isolation, a competition experiment does not provide conclusive evidence about the identity of the rate-determining step in a given reaction. However, additional context is provided by characterization of the catalyst resting state. Given that the selectivity-determining step must fall at or after the rate-determining step and that C–C bond-formation is the first step following from the resting state, the selectivity-determining (C_2H_4 vs. C_2D_4) and rate-determining steps coincide in this case. For further nuanced discussion, see: Simmons EM, Hartwig JF. Angew Chem Int Ed. 2012; 51:3066–3072.

51. Such a metal-centered and ligand-centered process has been characterized rigorously for the oxidative addition of biphenylene to pyridine(diimine) iron dinitrogen complexes. See: Darmon JM, Stieber SCE, Sylvester KT, Fernández I, Lobkovsky E, Semproni SP, Bill E, Wieghardt K, DeBeer S, Chirik PJ. J Am Chem Soc. 2012; 134:17125–17137. [PubMed: 23043331]

52. Representative procedures are reported here; for complete experimental details, see the Supporting Information.

53. Zhong AH, Labinger JA, Bercaw JE. J Am Chem Soc. 2002; 124:1378–1399. [PubMed: 11841307]

54. Wreford SS, Whitney JF. Inorg Chem. 1981; 20:3918–3942.

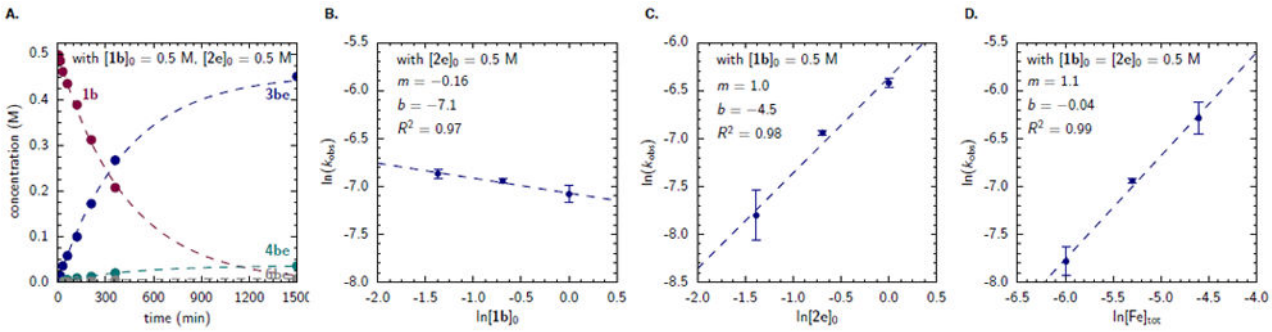

Figure 1.

Kinetic Analysis. A. The reaction time-course, wherein the concentrations of reactants and products are fit to an integrated first-order rate law, shows well-behaved kinetics with constant product selectivity over time. B–D. The approximately zero-order dependence on diene [**1b**], first-order dependence on alkene [**2e**], and first-order dependence on iron catalyst $[Fe]_{tot}$ were determined from initial rate measurements. All experiments conducted with $[Fe]_{tot} = [(^{Mes}DI)Fe(COD)]_{tot}$ = 5 mM unless noted otherwise.

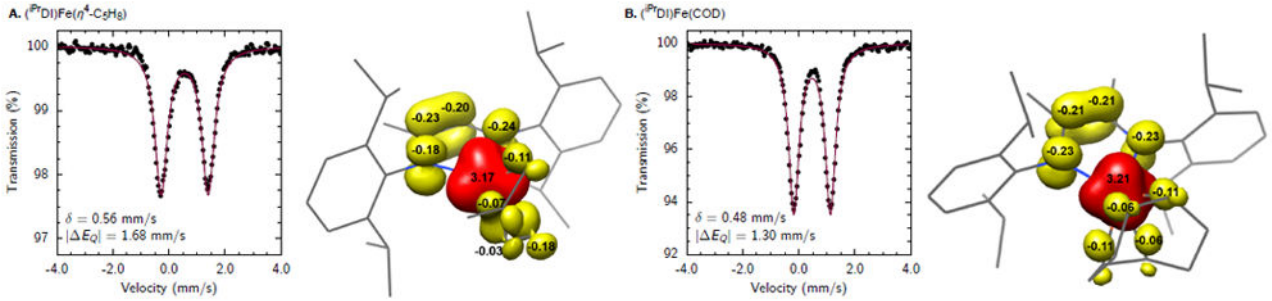

Figure 2.

Zero-field ^{57}Fe Mößbauer spectra (*left*) measured at 80 K, and spin-density plots (*right*) obtained from broken symmetry (3,1) Mulliken population analysis (red, positive spin density; yellow, negative spin density) calculated at the B3LYP level of theory.

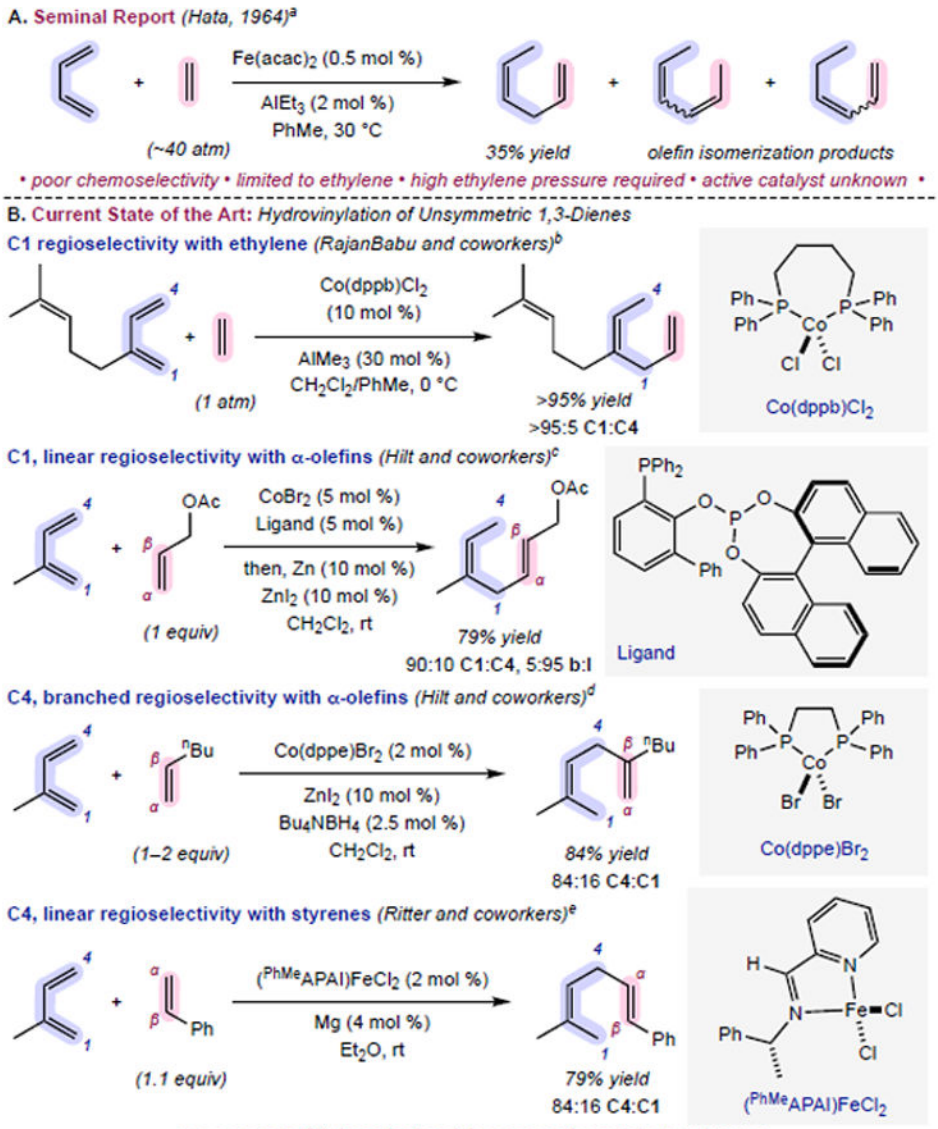

Scheme 1. State-of-the-art methods for selective [1,4]-hydrovinylation of 1,3-dienes rely on in situ catalyst activation

[a] See ref 6. [b] See ref 12d. [c] See ref 11k. The branched (**b**) product arises from C–C bond formation at Cβ; the linear (**l**) product arises from C–C bond formation at Cα. [d] See ref 11b. [e] See ref 14.

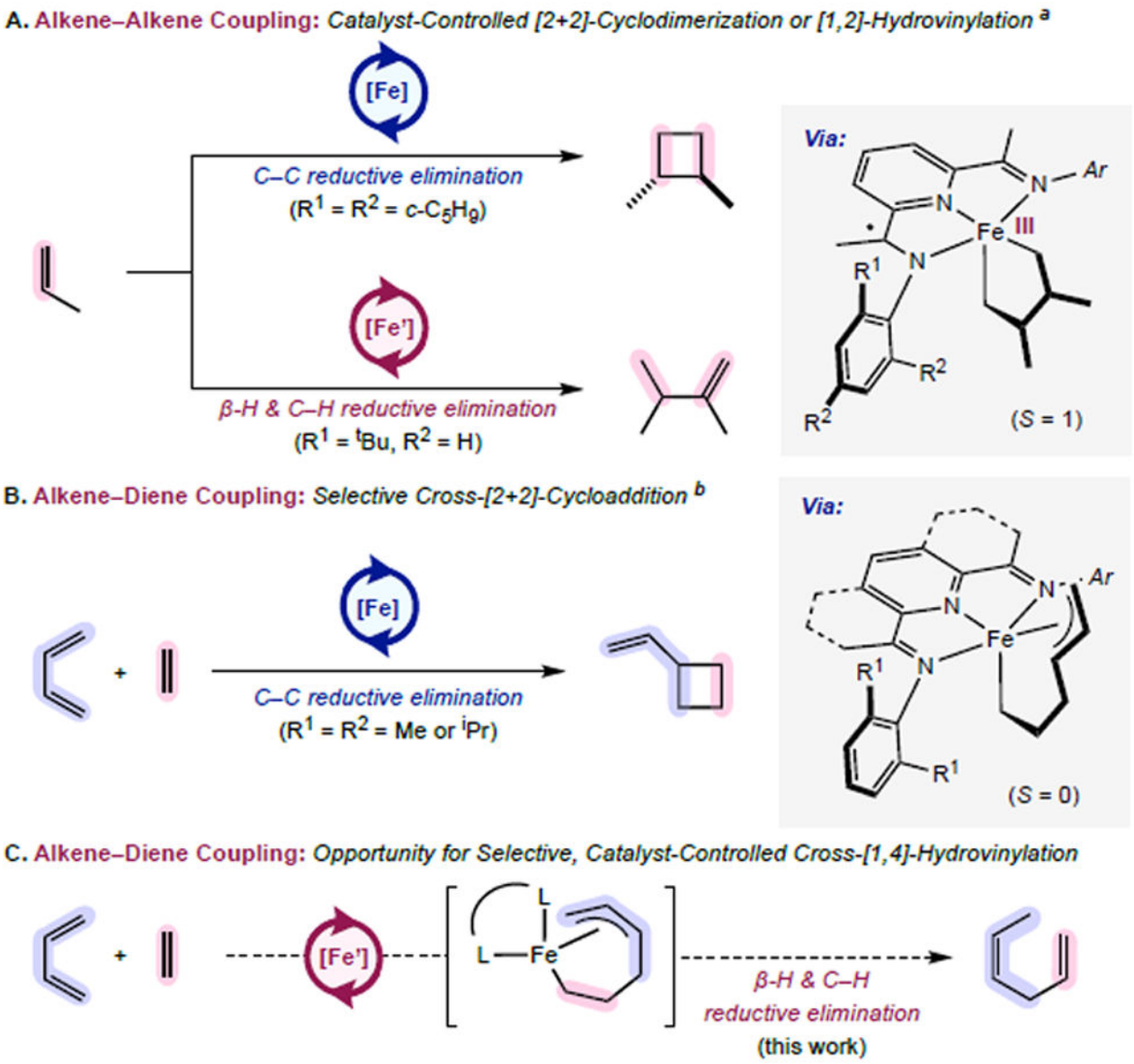

Scheme 2. Catalyst-controlled reactivity of metallacyclic intermediates allow selective access to value-added cyclic and acyclic hydrocarbons

[a] See refs 20 and 21. [b] See refs 20 and 24.

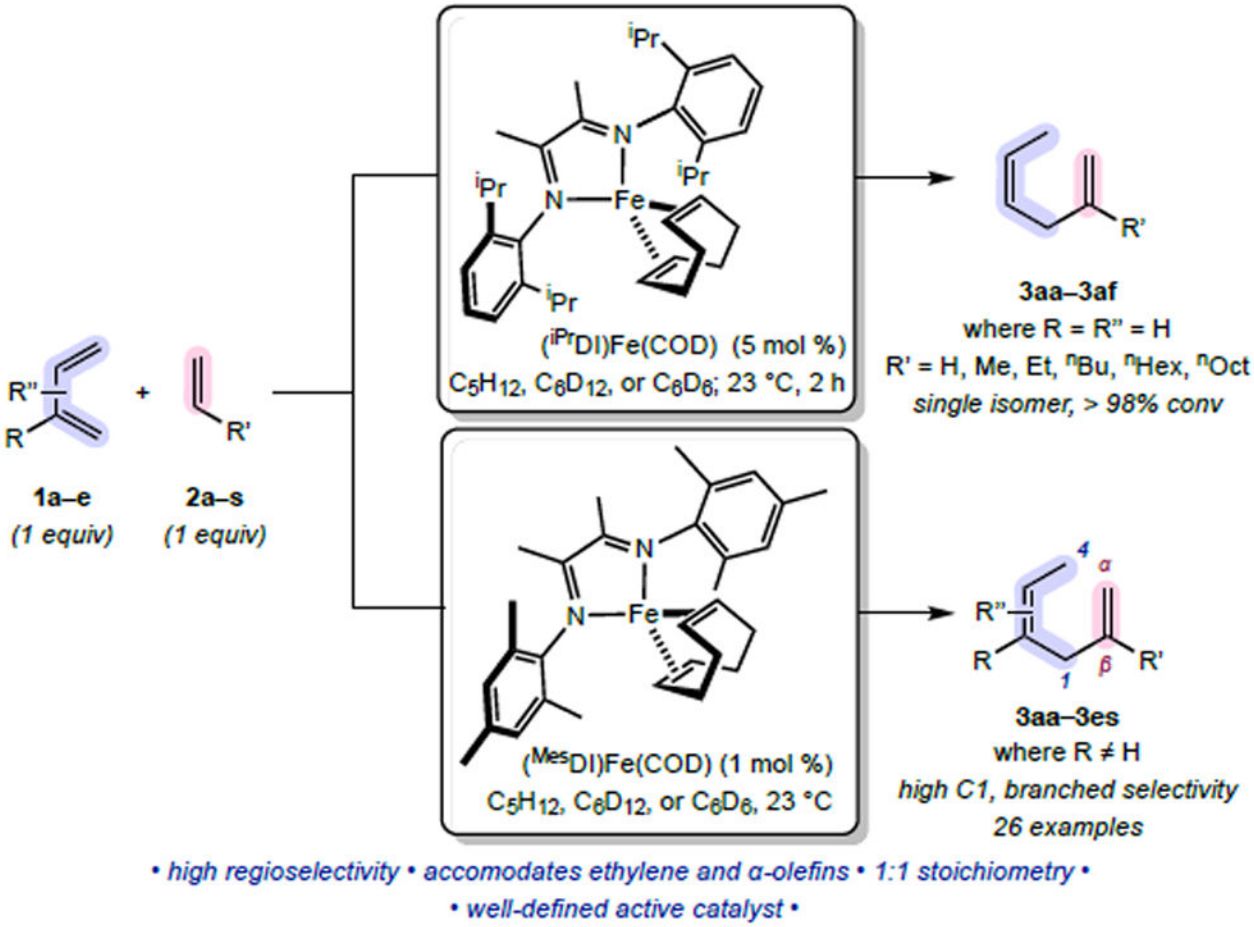

Scheme 3. Hydrovinylation of butadiene and substituted 1,3-dienes catalyzed by well-defined diimine iron complexes affords *C1, branched* products.[a]

[a] Linear hydrovinylation products and olefin isomers were not observed. Conversion was determined by ^{1}H NMR spectroscopy. Formation of the hydrovinylation cross products **3ab–af** (where R = R“ = H and R’ ≠ H) was accompanied by formation of 1,5-cyclooctadiene (up to 43% with respect to butadiene).

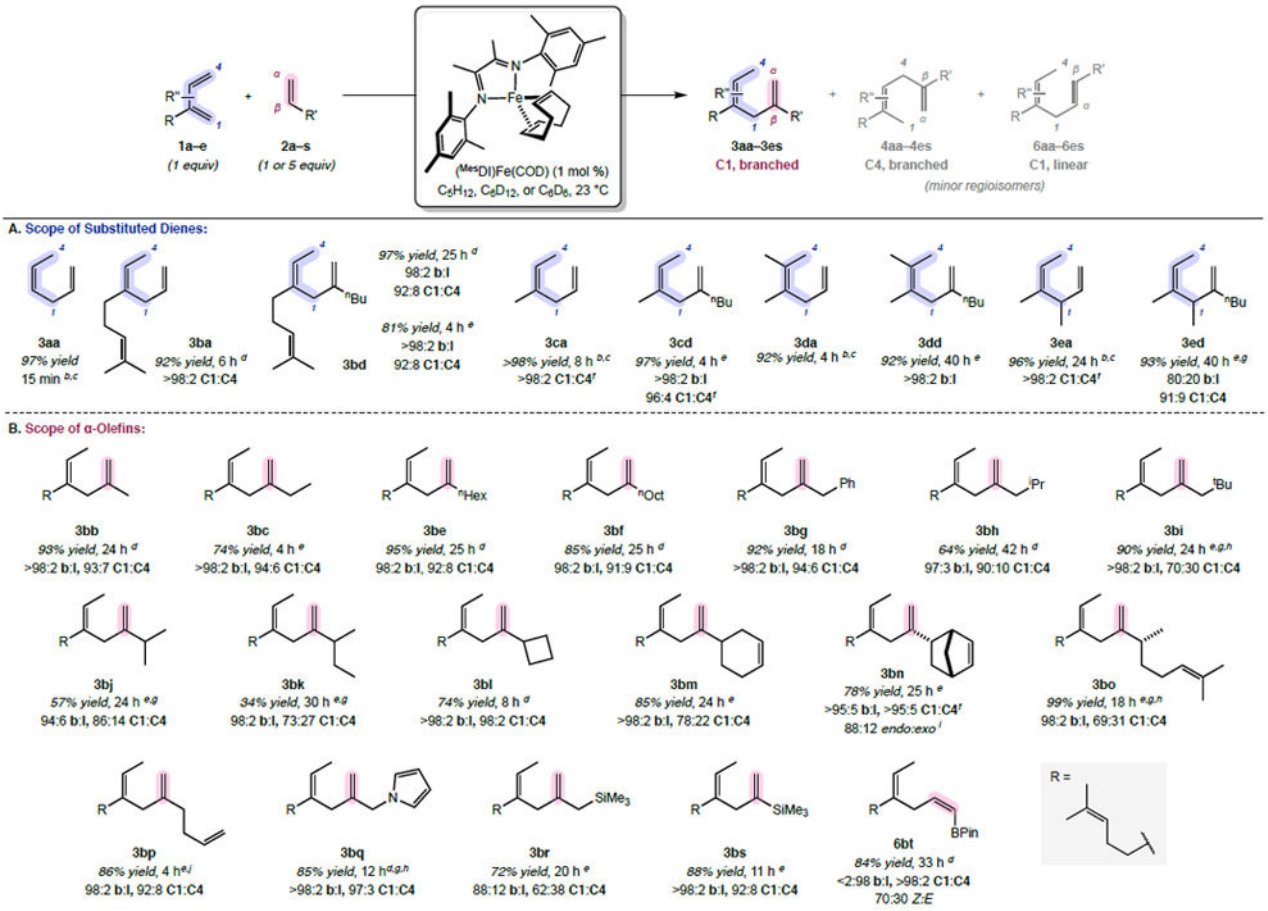

Scheme 4. Scope of [1,4]-Hydrovinylation.[a]

[a]Reactions monitored for consumption of diene **1** by gas chromatography. Combined yields listed for isomeric product mixtures isolated after the indicated time. Product ratios determined by gas chromatography unless noted otherwise. See the Supporting Information for a complete tabulation of substrates **1a–e** and **2a–t**. [b] Yield determined by ^{1}H NMR integration relative to an internal standard. [c] Reactions executed with 0.25 mmol 1 and 0.25 mmol **2** in C_6D_6 or C_6D_{12}. [d] Reactions executed with 0.5 mmol **1** and 0.5 mmol **2** in C_5H_{12}. [e] Reactions executed with 0.5 mmol **1** and 2.5 mmol **2** in C_5H_{12}. [f] Product ratios determined from relative ^{1}H NMR integration. [g] Unidentified isomeric products also formed: 7% of product mixture with **3ed**, 8% with **3bi**, 3% with **3bj**, 3% with **3bk**, 5% with **3bo**, and 7% with **3bq**. [h] Reaction run neat. [i] Using a 70:30 *endo:exo* mixture of 5-vinyl-2-norbornene isomers. [j] With 5% 2:1 myrcene–hexadiene adduct.

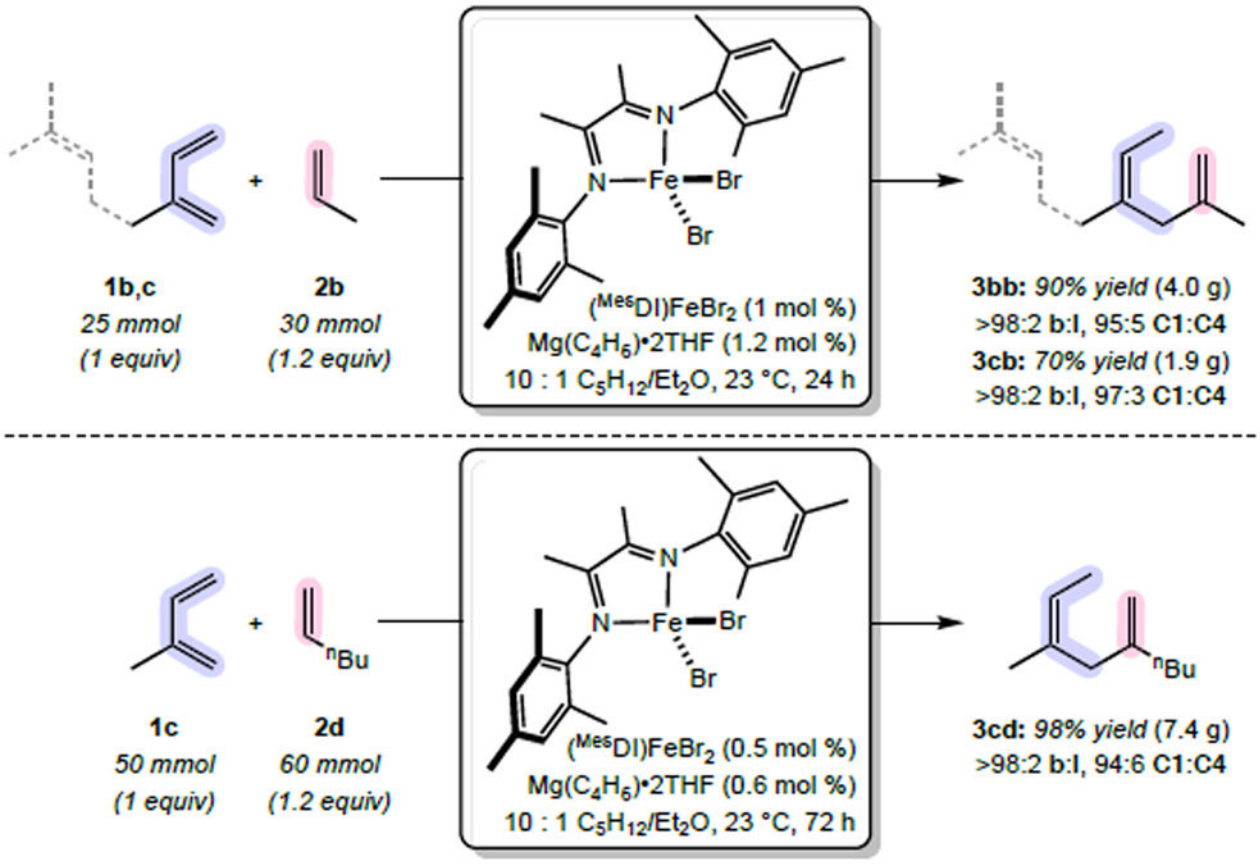

Scheme 5. In situ catalyst activation for multigram-scale, iron-atalyzed hydrovinylation reactions.[a]

[a]Combined yields listed for isomeric product mixtures isolated after the indicated time. Product ratios determined by gas chromatography.

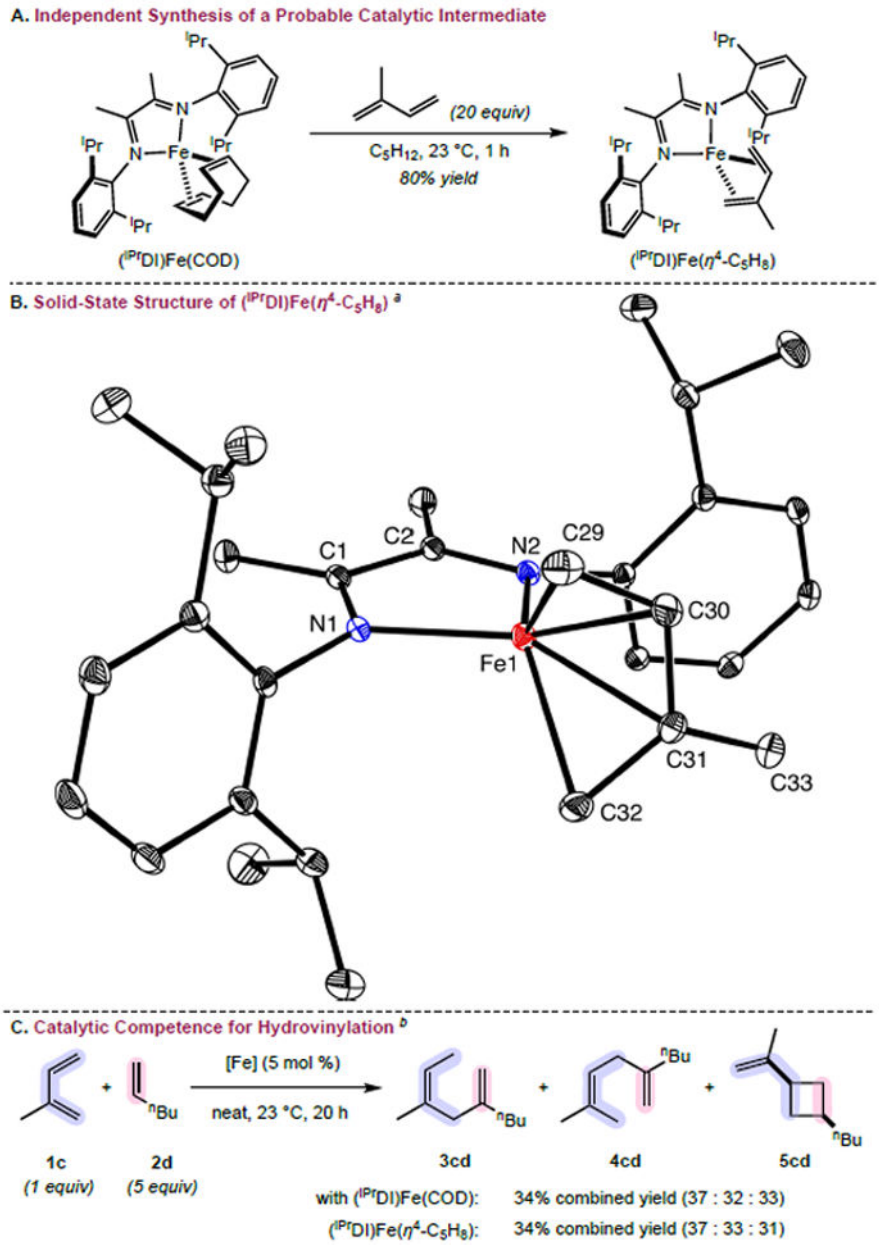

Scheme 6. Independent Synthesis and Structural Characterization of the Probable Catalyst Resting State

[a]Representation of the molecular structure of (^{iPr}DI)Fe(η^4-C_5H_8) with 30% probability ellipsoids. Hydrogen atoms and one isopropyl group omitted for clarity. [b]Combined yields listed for isomeric product mixtures isolated after the indicated time. Product ratios determined by gas chromatography.

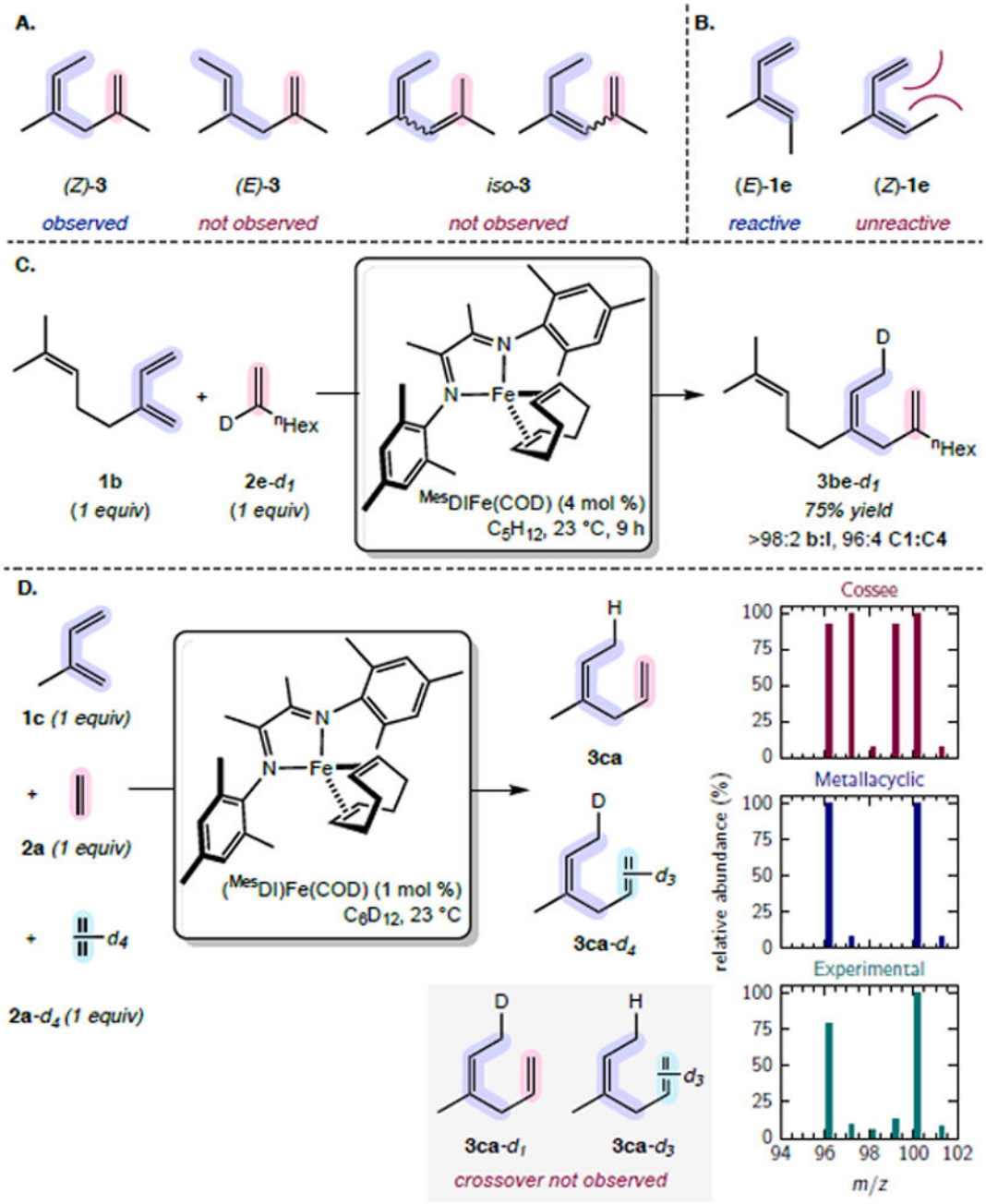

Scheme 7.

Evidence for On-Cycle Metallacycle Formation

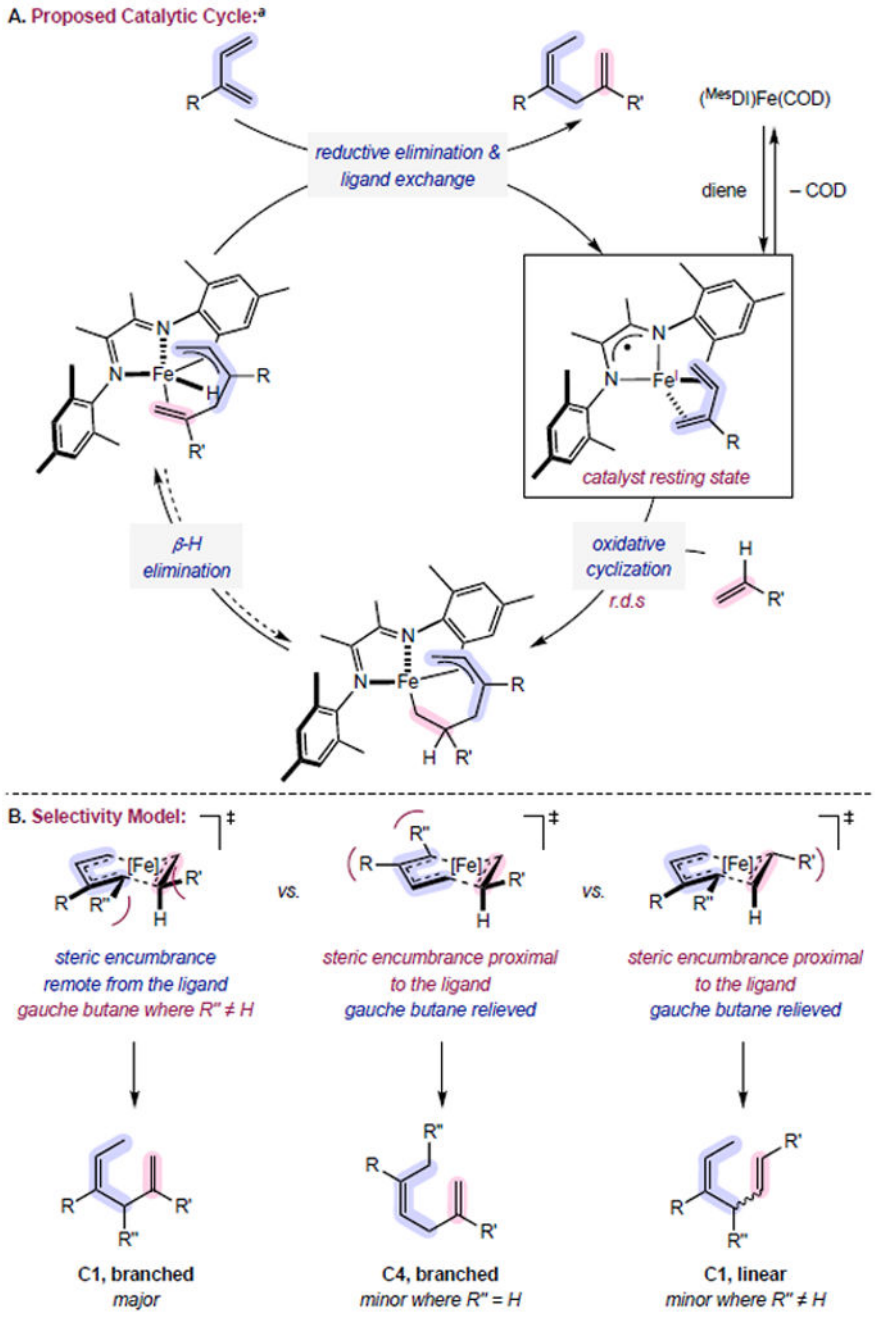

Scheme 8. Mechanistic Proposal

[a] The electronic structure, including ligand redox activity, is depicted explicitly only for the resting state iron diene complex. The neutral form of the diimine ligand is drawn in other cases to indicate that the electronic structure, which may or may not involve diimine ligand redox activity, is unknown. r.d.s. = rate-determining step

Table 1

Iron-catalyzed 1,4-hydrovinylation of myrcene with 1-hexene.[a]

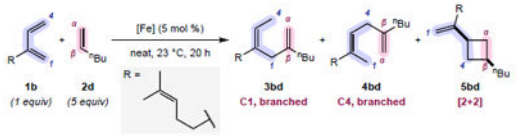

Entry	[Fe]	Conv[b]	Product Ratio[b]		
			3bd	4bd	5bd
1	[(^{Me}PDI)Fe(N_2)]$_2$(μ^2-N_2)	>98%	48	<1	52
2	($^{iPr(TB)}$PDI)Fe(N_2)$_2$	43%	<5	<1	>95
3	(^{iPr}DI)Fe(COE)	94%	73	1	21
4	(^{iPr}DI)Fe(COD)	93%	74	2	17
5	(^{C5H9}DI)Fe(COD)	98%	91	4	3
6	(^{Et}DI)Fe(COD)	>98%	95	3	2
7	(^{Mes}DI)Fe(COD)	>98%	95	5	<1
8	$FeCl_2$ + Mg(C_4H_6)•2THF[c]	<2% [d]	--	--	--

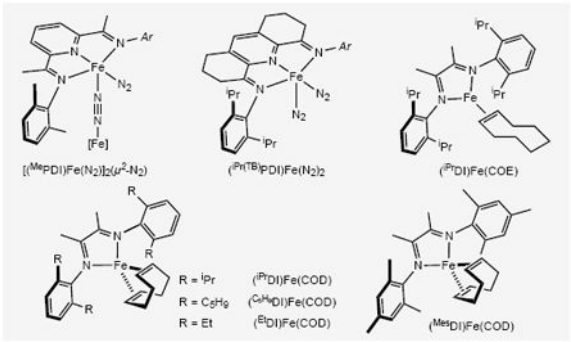

[a] Reactions executed with 0.2 mmol myrcene and 1.0 mmol 1-hexene at ambient temperature. Linear hydrovinylation products and olefin isomers not observed.

[b] Conversion (with respect to myrcene) and product ratio determined after 20 hours by gas chromatography.

[c] 5 mol% $Mg(C_4H_6)\cdot 2THF$ was added as an in situ reductant.

[d] Complex mixture of products.

Table 2

Select Bond Distances (Å) and Angles (°) for (^{iPr}DI)Fe(η^4-C_5H_8) and Related Structures.

	(^{iPr}DI)Fe(η^4-C_5H_8) [a]	(^{iPr}DI)Fe(COD) [b]	(^{C_5H_9}DI)Fe(COD) [c]	(^{Me}DI)Fe(COD) [d]	(^{R}DI$^{(ox)}$)^0 [e]	(^{R}DI$^{\bullet}$)$^{1-}$ [e]	(^{R}DI$^{(red)}$)$^{2-}$ [e]
Fe–N(1)	1.957(1)	1.9964(18)	1.991(2)	1.997(2)			
Fe–N(2)	1.966(2)	1.9944(18)	1.991(2)	1.988(2)			
N(1)–C(1)	1.343(2)	1.344(3)	1.344(3)	1.348(2)	1.29	1.35	1.38
N(2)–C(2)	1.340(2)	1.349(3)	1.3412(17)	1.346(2)	1.29	1.35	1.38
C(1)–C(2)	1.419(2)	1.413(3)	1.503(3)	1.411(2)	1.47	1.41	1.36
Fe–C(29)	2.136(2)	2.096(3)	2.0901(14)	2.091(2)			
Fe–C(30)	2.070(2)	2.115(3)	2.1235(13)	2.107(2)			
Fe–C(31)	2.091(2)						
Fe–C(32)	2.157(2)						
Fe–C(33)		2.105(2)	2.1240(14)	2.105(2)			
Fe–C(34)		2.082(2)	2.0733(14)	2.108(2)			
C(29)–C(30)	1.404(3)	1.375(6)	1.391(2)	1.397(3)			
C(30)–C(31)	1.440(3)						
C(31)–C(32)	1.404(3)						
C(33)–C(34)		1.397(2)	1.393(2)	1.401(2)			
N(1)–Fe–N(2)	80.31(6)	79.59(7)	79.82(4)	79.75(6)			

[a] See Scheme 6B.

[b] Taken from ref 29.

[c] See Supporting Information.

[d] Taken from ref 30.

[e] Taken from ref 28a where (^{R}DI$^{(ox)}$)^0 represents a generic diimine ligand in its neutral form, (^{R}DI$^{\bullet}$)$^{1-}$ represents a generic diimine ligand in its one-electron reduced radical monanionic form, and (^{R}DI$^{(red)}$)$^{2-}$ represents a generic diimine ligand in its closed-shell, two-electron reduced, dianionic form. Average values obtained from crystallographic analysis of diimine complexes with unambiguous ligand oxidation state assignments.

Table 3

Zero-Field ^{57}Fe Mößbauer Parameters for (^{iPr}DI)Fe(η^4-C_5H_8), (^{iPr}DI)Fe(COD), and Related Structures.[a]

[Fe]	δ (mm/s)	$\lvert\Delta E_Q\rvert$ (mm/s)	C.N. [b]	Oxidation state assignment	[Fe]	δ (mm/s)	$\lvert\Delta E_Q\rvert$ (mm/s)	C.N. [b]	Oxidation state assignment
(^{iPr}DI)Fe(η^4-C_5H_8)	0.56	1.68	4	Fe(I)	(^{Me}nacnac)Fe(NC^{t}Bu)$_2$ [g]	0.72	1.87	4	Fe(I)
BS(3,1) [c]	0.49	2.02			(^{Me}nacnac)Fe (4-^{t}Bu-Py)$_2$ [g]	0.79	0.59	4	Fe(I)–Fe(II) hybrid
(^{iPr}DI)Fe(COD)	0.48	1.30	4	Fe(I)					
(^{Mes}DI)Fe(COD)	0.46	0.98	4	Fe(I)	(^{Me}nacnac)FeBr(THF) [g]	0.89	2.36	4	Fe(II)
(^{Me}DI)Fe(COD) [d,e]	0.47	1.37	4	Fe(I)	(^{Me}nacnac)Fe(η^6-C_6H_6) [g]	0.70	0.74	5	Fe(I)
	0.44	0.88	4	Fe(I)					
(^{iPr}DI)FeCl$_2$ [f]	0.84	2.57	4	Fe(II)	($^{iPr(TB)}$PDI)Fe(N$_2$)$_2$ [h]	0.45	0.83	5	Fe(0)–Fe(II) hybrid
(^{iPr}DI)$_2$Fe [f]	0.77	1.81	4	Fe(II)					
(^{Me}DI)Fe (η^6-$C_6H_5CH_3$) [d]	0.44	0.27	5	Fe(0)–Fe(II) hybrid	($^{iPr(TB)}$PDI)Fe (η^2,η^2-((CH$_2$CHCH$_2$)$_2$) [h]	0.73	1.81	5	Fe(I)

[a] All measurements recorded at 80 K. Complete ligand structures for all listed complexes depicted in the Supporting Information.

[b] Coordination number.

[c] Calculated using the broken symmetry solution for the electronic structure of (^{iPr}DI)Fe(η^4-C_5H_8) determined using DFT.

[d] Taken from ref 30.

[e] Two polymorphs characterized independently.

[f] Taken from ref 28.

[g] Taken from ref 38.

[h] Taken from ref 21; see Table 1 for ligand structure.